THE JOURNAL OF BIOLOGICAL CHEMISTRY
Vol. 279, No. 18, Issue of April 30, pp. 18440–18450, 2004
Printed in U.S.A.

The Coxsackievirus 2B Protein Suppresses Apoptotic Host Cell Responses by Manipulating Intracellular Ca^{2+} Homeostasis*

Received for publication, August 27, 2003, and in revised form, February 5, 2004
Published, JBC Papers in Press, February 19, 2004, DOI 10.1074/jbc.M309494200

Michelangelo Campanella‡, Arjan S. de Jong§, Kjerstin W. H. Lanke§, Willem J. G. Melchers§, Peter H. G. M. Willems¶, Paolo Pinton‡, Rosario Rizzuto‡‖, and Frank J. M. van Kuppeveld§**

From the ‡Department of Experimental and Diagnostic Medicine, Section of General Pathology and Center for the Study of Inflammatory Diseases, Via Borsari 46, I-44100 Ferrara, Italy and the Departments of §Medical Microbiology and ¶Biochemistry, Nijmegen Center for Molecular Life Sciences, University Medical Center Nijmegen, P.O. Box 9101, 6500 HB Nijmegen, The Netherlands

Enteroviruses, small cytolytic RNA viruses, confer an antiapoptotic state to infected cells in order to suppress infection-limiting apoptotic host cell responses. This antiapoptotic state also lends protection against cell death induced by metabolic inhibitors like actinomycin D and cycloheximide. The identity of the viral antiapoptotic protein and the underlying mechanism are unknown. Here, we provide evidence that the coxsackievirus 2B protein modulates apoptosis by manipulating intracellular Ca^{2+} homeostasis. Using fluorescent Ca^{2+} indicators and organelle-targeted aequorins, we demonstrate that ectopic expression of 2B in HeLa cells decreases the Ca^{2+} content of both the endoplasmic reticulum and the Golgi, resulting in down-regulation of Ca^{2+} signaling between these stores and the mitochondria, and increases the influx of extracellular Ca^{2+}. In our studies of the physiological importance of the 2B-induced alterations in Ca^{2+} signaling, we found that the expression of 2B suppressed caspase activation and apoptotic cell death induced by various stimuli, including actinomycin D and cycloheximide. Mutants of 2B that were defective in reducing the Ca^{2+} content of the stores failed to suppress apoptosis. These data implicate a functional role of the perturbation of intracellular Ca^{2+} compartmentalization in the enteroviral strategy to suppress intrinsic apoptotic host cell responses. The putative down-regulation of an endoplasmic reticulum-dependent apoptotic pathway is discussed.

Many viruses are endowed with the potential to manipulate cell death pathways in order to prevent premature abortion of the infectious cycle (1, 2). The molecular mechanism by which enteroviruses manipulate the life span of their host cell is, as yet, poorly understood. Enteroviruses (coxsackievirus, poliovirus, and ECHO virus) are nonenveloped, cytolytic RNA viruses that replicate their genome at the secretory pathway-derived membrane vesicles that accumulate in the cytoplasm of the infected cell (3). Classically, lytic viral replication is believed to induce canonical cellular necrosis by destruction of the plasma membrane, causing the collapse of ionic gradients. However, evidence is accumulating that the issue of how enteroviruses induce cell death is much more complex. Enterovirus infection leads to the development of the so-called cytopathic effect (CPE),[1] a necrosis-like type of cell death that is characterized by rounding up of the infected cells, distortion and displacement of the nuclei, condensation of chromatin, and increased plasma membrane permeability. This type of cell death is the result of a complex interplay between apoptosis-inducing and apoptosis-suppressing functions encoded by the enterovirus genome (4–6). Early in infection, *i.e.* upon translation of the enterovirus RNA genome, sufficient quantities of a putative pro-apoptotic function are produced to trigger an apoptotic response. Concomitantly with the onset of viral replication, however, the implementation of the virus-induced apoptotic program is abruptly interrupted, suggesting that enteroviruses also encode an antiapoptotic function (6). This antiapoptotic function also renders infected cells resistant against non-viral apoptotic stimuli like cycloheximide and actinomycin D (4). The apoptosis-suppressing function dominates upon productive infection (*i.e.* conditions that allow efficient virus replication). Under these conditions, only at late stages (*i.e.* after the development of CPE) can some signs of apoptosis be detected (7). Virus replication and CPE, however, are not sensitive to caspase inhibitors or the overexpression of Bcl-2 (5). The apoptosis-inducing function dominates upon non-permissive infection (*i.e.* conditions that restrict virus growth). The full-blown apoptosis that is induced under these latter conditions is efficiently suppressed by caspase inhibitors as well as by Bcl-2 overexpression (5).

Recent studies have shed some light on the identity of the putative apoptosis-inducing enterovirus proteins. Individual expression of the viral proteinase $2A^{pro}$, which inhibits cap-dependent translation of cellular mRNAs, or the expression of $3C^{pro}$, which shuts off host cell RNA transcription, results in apoptotic cell death (8, 9). Little is known about the identity of the apoptosis-suppressing factors. The 3A protein suppresses the extrinsic apoptotic pathway by eliminating labile receptors

* This research was partly supported by the Netherlands Organization for Scientific Research Grant NOW-917.46.305 (to F. J. M. v. K.), European Communities Grant INTAS-01-2012 (to W. J. G. M.), Telethon-Italy Grants 1285 and GTF02013 (to R. R.), and grants from the Italian Association for Cancer Research (AIRC), the Human Frontier Science Program, the Italian University Ministry (MURST and FIRB), and the Italian Space Agency (ASI) (to R. R.). The costs of publication of this article were defrayed in part by the payment of page charges. This article must therefore be hereby marked "*advertisement*" in accordance with 18 U.S.C. Section 1734 solely to indicate this fact.

‖ To whom correspondence may be addressed. Tel.: 39-0532-291361; Fax: 39-0532-247278; E-mail: r.rizzuto@unife.it.

** To whom correspondence may be addressed. Tel.: 31-24-3617574; Fax: 31-24-3614666; E-mail: f.vankuppeveld@ncmls.kun.nl.

[1] The abbreviations used are: CPE, cytopathic effect; ER, endoplasmic reticulum; aa, amino acid(s); DAPI, 4′,6-diamidino-2-phenylindole; KRB, Krebs-Ringer buffer; DMEM, Dulbecco's modified Eagle's medium; FBS, fetal bovine serum; CHO, Chinese hamster ovary; GFP, green fluorescent protein; EGFP, enhanced GFP; AEQ, aequorin; cyt, cytosolic; er, ER-targeted; Go, Golgi-targeted; mt, mitochondrially targeted; IP3, inositol 1,4,5-trisphosphate; GuHCl, guanidine hydrochloride.

from the cell surface (10) through its ability to inhibit protein secretion (11). The enteroviral protein that is responsible for the suppression of the intrinsic apoptotic host cell responses has not yet been identified.

Ca^{2+} is one of the most versatile and universal signaling mediators in cells and is required for the activation of many cellular processes. Increasing evidence indicates that alterations in the finely tuned intracellular Ca^{2+} homeostasis and compartmentalization can lead to cell death, either through apoptosis or necrosis (12). The switch from the control of physiological functions to the death program most likely involves alterations in the tightly regulated spatio-temporal Ca^{2+} pattern or alterations at the level of organelles (*e.g.* mitochondria or ER/Golgi) or effector proteins (*e.g.* calpain or calcineurin) that are activated by Ca^{2+} (13). Enteroviruses have a profound effect on intracellular Ca^{2+} homeostasis (14, 15). We have previously shown that infection of HeLa cells with the coxsackievirus results in a reduction of the amount of Ca^{2+} that can be released from the intracellular stores. In parallel, a gradual increase in the cytosolic Ca^{2+} concentration ($[Ca^{2+}]_{cyt}$) is observed due to the influx of extracellular Ca^{2+} (15).

The enterovirus 2B protein has been implicated in the virus-induced alterations in intracellular Ca^{2+} homeostasis (15, 16). The 2B protein is a small (97–99 aa) membrane-integral replication protein (17) that, in infected cells, is localized at the surface of the ER- and Golgi-derived membrane vesicles at which viral replication takes place (3, 18, 19). All enterovirus 2B proteins contain two hydrophobic regions, of which one is predicted to form a cationic amphipathic α-helix (20, 21). This amphipathic α-helix displays characteristics typical for the group of membrane-lytic α-helical peptides that can build membrane-integral pores by forming multimeric transmembrane bundles (22, 23). Homomultimerization reactions of 2B have been demonstrated by yeast and mammalian two-hybrid (24, 25) and biochemical approaches (26) and in living cells by using fluorescence resonance energy transfer (FRET) microscopy (27). These data strongly suggest that 2B is responsible for the reduction of the $[Ca^{2+}]$ in ER and Golgi ($[Ca^{2+}]_{ER}$ and $[Ca^{2+}]_{Golgi}$) by building pores in the membranes of these organelles. Direct evidence that 2B indeed causes a reduction in the $[Ca^{2+}]$ of the stores is, however, still lacking.

In this study, we investigated Ca^{2+} homeostasis in 2B-expressing cells and evaluated the physiological importance of the alterations in Ca^{2+} signaling for the implementation or suppression of the different cell death programs. Using fluorescent Ca^{2+} indicators and organelle-targeted aequorins (AEQs; genetically encoded Ca^{2+} sensors), we demonstrate that 2B indeed reduces $[Ca^{2+}]_{ER}$ and $[Ca^{2+}]_{Golgi}$ in HeLa cells. We show that this leads to a decrease in the amount of Ca^{2+} that can be released from these stores and, as a consequence, results in the stimulus-induced rise of $[Ca^{2+}]$ in the mitochondria ($[Ca^{2+}]_{mt}$). Moreover, the influx of Ca^{2+} from the extracellular medium is increased, and, thus, the $[Ca^{2+}]_{cyt}$ responses are larger. In our studies of the functional importance of the 2B-induced manipulation of intracellular Ca^{2+} signaling, we found that the expression of 2B suppressed apoptosis induced by certain stimuli, including actinomycin D and cycloheximide. 2B mutants that were unable to reduce the Ca^{2+} content of the stores failed to protect against apoptosis. These data implicate a functional role of the 2B-induced perturbation of intracellular Ca^{2+} compartmentalization in the enteroviral strategy to suppress premature abortion of the viral life cycle and provide a physiological example of the regulatory role of Ca^{2+} signaling in the modulation of apoptotic cell death.

EXPERIMENTAL PROCEDURES

Reagents and Solutions—Fura-2/AM and coelenterazine were purchased from Molecular Probes (Leiden, The Netherlands). Thapsigargin, histamine, actinomycin D, cycloheximide *N*-acetyl-D-sphingosine (C_2 ceramide), and etoposide were purchased from Sigma. DAPI was obtained from Merck. HT buffer contained 132.6 mM NaCl, 5.5 mM glucose-monohydrate, 10 mM HEPES, 4.2 mM $MgCl_2$, and (1×) minimum Eagle's medium amino acids (Invitrogen). Krebs-Ringer buffer (KRB) contained 20 mM HEPES pH 7.4, 125 mM NaCl, 5 mM KCl, 1 mM $MgSO_4$, 1 mM Ha_2HPO_4, 20 mM $NaHCO_3$, 5.5 mM glucose, and 2 mM L-glutamine.

Cell Culture, Viruses, Plasmids, and Transfection—HeLa cells were grown in DMEM (Life Technologies, Inc.) supplemented with 10% FBS, 100 units/ml penicillin, and 25 μg/ml streptomycin. CHO cells were grown in DMEM supplemented with 10% FBS and 100 μg/ml gentamycin. Cells were grown at 37 °C in a 5% CO_2 incubator.

The coxsackievirus B3 used in this study was derived from plasmid pCB3/T7, which contains a cDNA of coxsackievirus B3 (strain Nancy) behind a T7 RNA polymerase promoter. Virus titers were determined by end point titration as described (20).

Plasmid GFP (S65T) was from Clontech. Plasmid 2B-GFP (S65T) was constructed by replacing the enhanced cyan fluorescent protein (ECFP) coding region from 2B-ECFP (27) with the GFP (S65T) coding region using AgeI and BfrI. Plasmid 2B-EGFP has been described (17). Plasmid mt-GFP encodes an EGFP protein that is targeted to the mitochondria through fusion with the signal sequence of cytochrome oxidase subunit VIII (28). ER-targeted aequorin (erAEQ), Golgi-targeted aequorin (GoAEQ), mitochondrially targeted aequorin (mtAEQ), and cytosolic aequorin (cytAEQ) have been described (29–32).

For the Fura-2/AM measurements, 3×10^5 CHO cells were transfected with 2 μg of either GFP (S65T) or 2B-GFP (S65T) using Lipofectin (Invitrogen). After 24 h, 5×10^4 cells were seeded onto 24-mm coverslips and grown for another 16 h before $[Ca^{2+}]_{cyt}$ measurements. For the aequorin measurements, HeLa cells were seeded onto 13-mm coverslips and cotransfected using the Ca^{2+} phosphate technique with 1 μg of erAEQ, GoAEQ, cytAEQ, or mtAEQ, together with 3 μg of 2B-EGFP or in combination with the same amount (3 μg) of mt-GFP (which served as negative control). For the cell death experiments, HeLa cells were seeded onto 24-mm coverslips and transfected with 4 μg of 2B-EGFP or mt-GFP.

Fura-2/AM Measurements—The fluorescent Ca^{2+} indicator Fura-2 was used to measure $[Ca^{2+}]_{cyt}$ at the single cell level essentially as described (15). Briefly, cells were incubated in medium supplemented with 2.5 μM Fura-2/AM for 30 min, washed with HT buffer to remove the extracellular probe, supplied with preheated HT buffer (supplemented with 1 mM $CaCl_2$), and placed in a thermostated (37 °C) incubation chamber on the stage of an inverted fluorescence microscope (Nikon). Dynamic video imaging was performed using the MagiCal hardware and TARDIS software (Joyce Loebl, Tyne and Wear, UK). Fluorescence was measured every 2 s with the excitation wavelength alternating between 340 and 380 nm and the emission fluorescence being recorded at 492 nm. At the end of the experiment, a region free of cells was selected, and one averaged background frame was collected at each excitation wavelength for background correction. To measure the $[Ca^{2+}]$ of the stores, the amount of thapsigargin-releasable Ca^{2+} was determined. After recording the cells in Ca^{2+}-containing HT buffer, the medium was replaced with Ca^{2+}-free HT buffer supplemented with 0.5 mM EGTA. After 10 min, the cells were challenged with 1 μM thapsigargin, and $[Ca^{2+}]_{cyt}$ was measured as described above.

Aequorin Measurements—Organelle-targeted aequorin constructs were used to measure the $[Ca^{2+}]$ in the cytosol and different organelles at the cell population level (at 36 h post-transfection). For the mtAEQ and cytAEQ measurements, the cells were incubated with 5 μM coelenterazine for 1–2 h in DMEM supplemented with 1% FBS and then transferred to the perfusion chamber. To reconstitute the erAEQ and GoAEQ with high efficiency, the luminal $[Ca^{2+}]$ of the ER and Golgi first must be reduced. This was achieved by incubating the cells for 1 h at 4 °C in KRB supplemented with 5 μM coelenterazine, the Ca^{2+} ionophore ionomycin, and 600 μM EGTA. After this incubation, cells were extensively washed with KRB supplemented with 2% bovine serum albumin. The coverslip with transfected cells was placed in a perfused, thermostated chamber located in the close proximity of a low noise photomultiplier, with built-in amplifier-discriminator. All aequorin measurements were carried out in KRB supplemented with either 1 mM Ca^{2+} or the indicated $[Ca^{2+}]$. Agonists and other drugs were added to the same medium, as specified in the relevant figure legends. The experiments were terminated by lysing the cells with 100

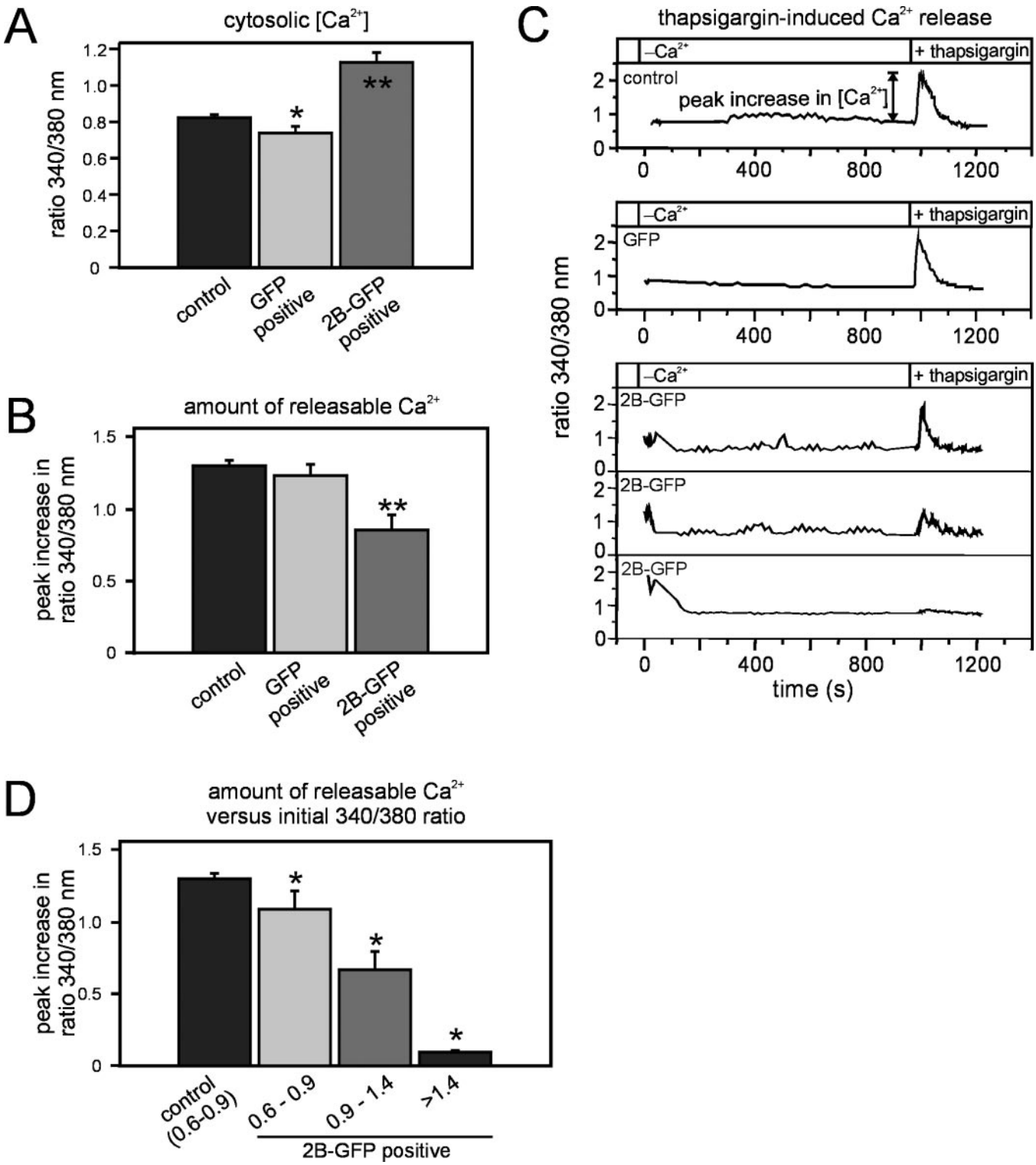

FIG. 1. **Intracellular Ca^{2+} homeostasis in 2B-expressing cells.** *A*, $[Ca^{2+}]_{cyt}$ of CHO cells expressing GFP or 2B-GFP at 48 h posttransfection. Cells were loaded with Fura-2/AM, GFP-positive cells were identified, the fluorescence at 340 and 380 nm was analyzed, and the ratio 340/380 nm was calculated. *B*, the amount of thapsigargin-releasable Ca^{2+}. The average peak increase in the thapsigargin-induced 340/380 nm ratio is shown (*i.e.* the increase in the 340/380 nm ratio relative to the basal 340/380 nm ratio in the Ca^{2+}-free medium that was recorded just before the addition of thapsigargin; see *panel C*). *C*, representative traces showing the peak increases in thapsigargin response of a control cell, a GFP expressing cell, and three 2B-GFP expressing cells. *D*, average peak increase in the thapsigargin-induced 340/380-nm ratio plotted against the initial 340/380-nm ratio of cells in the presence of extracellular Ca^{2+}. Note that the average amount of thapsigargin-releasable Ca^{2+} of 2B-GFP-expressing cells that exhibited an initial 340/380-nm ratio of 0.6–0.9 (which is similar to that of the control cells) was significantly lower than that of control cells. In each experiment, the 340/380-nm ratio of a large number of cells from different coverslips was analyzed. The average ± S.D. of five independent experiments is shown. *, $p < 0.05$; **, $p < 0.01$.

μM digitonin in a hypotonic Ca^{2+}-containing solution (10 mM $CaCl_2$ in H_2O), thus discharging the remaining aequorin pool. The output of the discriminator was captured by a Thorn-EMI photon counting board and stored in an IBM-compatible computer for further analyses. The aequorin luminescence data were calibrated off-line into $[Ca^{2+}]$ values, using a computer algorithm based on the Ca^{2+} response curve of wild-

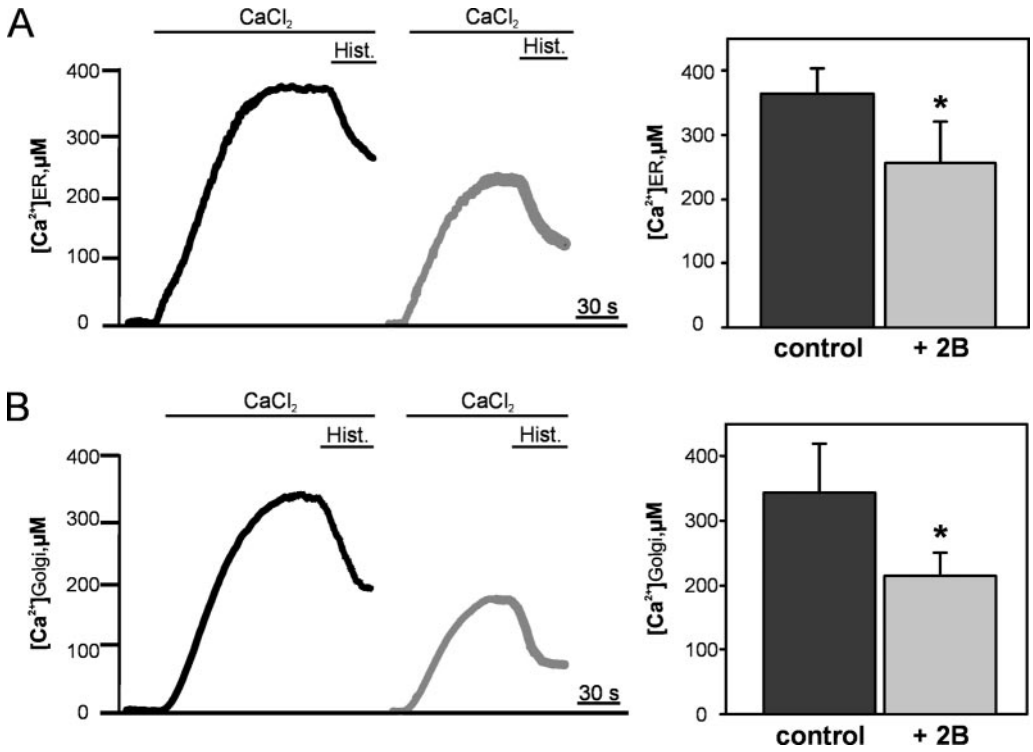

FIG. 2. **$[Ca^{2+}]_{ER}$ and $[Ca^{2+}]_{Golgi}$ in 2B-expressing cells.** HeLa cells were cotransfected with ER-targeted or Golgi-targeted aequorin (erAEQ or GoAEQ, respectively) and 2B-GFP or mt-GFP (control). At 36 h posttransfection, the organelles were depleted of Ca^{2+} to optimize AEQ reconstitution. After this, the cells were transferred to the luminometer chamber, and AEQ luminescence was collected and calibrated into $[Ca^{2+}]$ values as described under "Experimental Procedures." Representative traces of $[Ca^{2+}]_{ER}$ (*A*) and $[Ca^{2+}]_{Golgi}$ (*B*) in 2B-expressing cells (*gray line*) and control cells (*black line*) are shown on the *left*. On the *right* is shown the average ± S.D. of ten independent experiments. *, $p < 0.005$. *Hist.*, histamine.

type and mutant aequorins (30, 33).

Cell Death Analysis—To assay the antiapoptotic effects in coxsackievirus-infected cells, cells grown on coverslips were either mock-infected or infected with coxsackievirus (30 min at room temperature) at a multiplicity of infection of 50. At the indicated times (specified in the relevant figure legends), cells were challenged with guanidine hydrochloride (GuHCl) (2 mM), cycloheximide (100 μg/ml), or actinomycin D (0.5 μg/ml) for the indicated times. For the analysis of the nuclear morphology, cells were fixed with 4% paraformaldehyde, stained with DAPI (10 μg/ml), viewed under an Axiovert epifluorescence-inverted microscope (Carl-Zeiss GmbH), and imaged with a Nikon Coolpix 995 digital camera equipped with an MDC lens. Caspase activation was analyzed using the Apo-ONE™ homogeneous caspase-3/7 assay according to the instructions of the manufacturer (Promega). Analysis of DNA fragmentation was performed as described by Tolskaya *et al.* (4). Incubations were performed in serum-free DMEM except for the experiments in which caspase-3 activation was assayed (because of the high caspase-3 background in serum-free DMEM in control cells and infected cells).

To investigate the antiapoptotic effects in 2B-expressing cells, cells grown on coverslips were transfected either with 2B-GFP or mt-GFP. At 36 h post-transfection, cells were treated with the apoptosis-inducing drugs for 4 h (for analysis of caspase-3 activation) or 16 h (for analysis of cell survival). Incubation with cycloheximide, actinomycin D, and etoposide was performed in DMEM containing 10% FBS. Incubation with ceramide was performed in KRB buffer supplemented with 1 mM $CaCl_2$. To assay caspase-3 activation, cells were fixed and stained as described (17) with an anti-cleaved caspase-3 (Asp-175) antibody (Cell Signaling Technology), which specifically recognizes active caspase-3 but not its inactive zymogen, and a Texas Red-conjugated goat anti-rabbit antibody. The percentage of caspase-3-positive GFP-expressing cells was determined *de visu* by counting at the microscope. To assay cell survival, cells were washed thoroughly to eliminate apoptotic cells after incubation with the apoptotic drugs. The percentage of fluorescent cells before and after a challenge with the apoptotic drugs was determined *de visu* by counting at the microscope.

RESULTS

Ca^{2+} Homeostasis in 2B-expressing Cells—To investigate the effects of 2B on subcellular Ca^{2+} homeostasis, we made use of a fusion protein of 2B and GFP. We have shown previously that the fusion of EGFP at the C terminus of the coxsackievirus 2B protein does not interfere with its membrane-active function and localization (17). Because the EGFP fluorescence heavily contaminates that of the fluorescent Ca^{2+} indicator Fura-2 (data not shown) (34), we made use of GFP (S65T), a non-enhanced GFP protein that exhibits 30-fold reduced fluorescence intensity relative to EGFP. Fig. 1*A* shows the $[Ca^{2+}]_{cyt}$ of nontransfected control cells and cells expressing either GFP (S65T) or 2B-GFP (S65T). The $[Ca^{2+}]_{cyt}$ in GFP-expressing cells was slightly lower than that of control cells (suggesting that there is some minor contamination of the Fura-2 fluorescence by GFP). Expression of 2B-GFP, however, resulted in a significant increase in $[Ca^{2+}]_{cyt}$ ($p < 0.01$), shown previously to depend on extracellular Ca^{2+} (15).

Next, we addressed the relationship between the $[Ca^{2+}]_{cyt}$ and the $[Ca^{2+}]$ of the intracellular stores (*i.e.* ER and Golgi) using thapsigargin, a specific inhibitor of the sarco/endoplasmic reticulum Ca^{2+} ATPase (SERCA) pump. The activity of the SERCA is required to compensate for the continuous leakage of Ca^{2+} that takes place from the stores under normal conditions. Upon inhibition of the SERCA, the Ca^{2+} that leaks from the stores is not resequestered and accumulates in the cytosol. The size of the thapsigargin-induced transient increase in $[Ca^{2+}]_{cyt}$ reflects the $[Ca^{2+}]$ of the stores. Fig. 1*B* shows that the amount of thapsigargin-releasable Ca^{2+} in cells expressing GFP was similar to that observed in nontransfected control cells. Cells expressing 2B-GFP, however, exhibited a significant decrease ($p < 0.01$) in the amount of thapsigargin-releasable Ca^{2+}. Fig. 1*C* shows representative traces of nontransfected controls cells, cells expressing GFP, and cells expressing 2B-GFP. The amount of thapsigargin-releasable Ca^{2+} from cells expressing 2B-GFP exhibited an inverse relationship with the initial $[Ca^{2+}]_{cyt}$ (as measured in the presence of extracellular Ca^{2+});

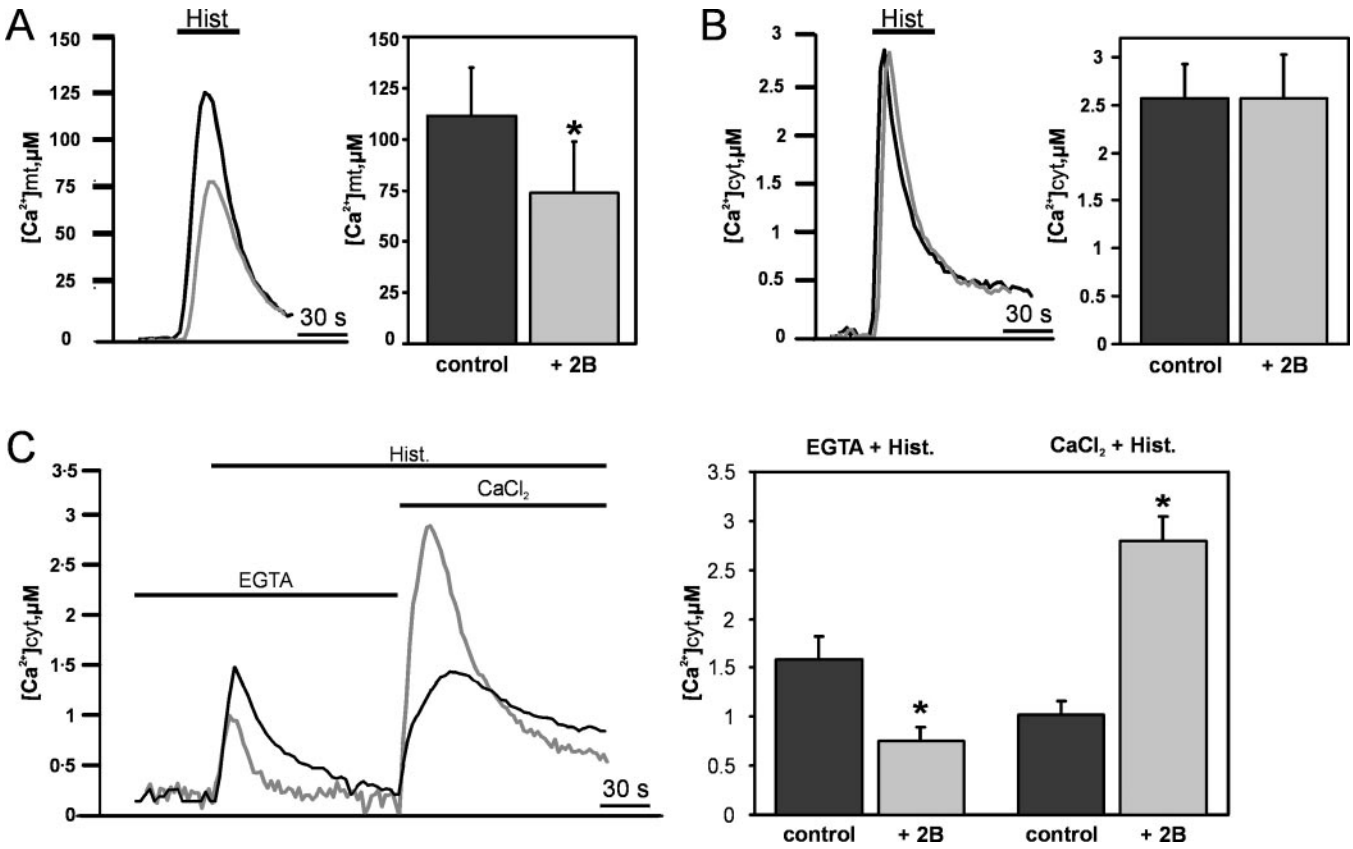

FIG. 3. **Stimulus-induced increases in $[Ca^{2+}]_{mt}$ and $[Ca^{2+}]_{cyt}$ in 2B-expressing cells.** HeLa cells were cotransfected with mitochondrially targeted (*A*) or cytosolic aequorin (*B*) (mtAEQ or AEQ, respectively) and 2B-GFP or mt-GFP (control), incubated in medium containing extracellular Ca^{2+}, and then challenged with 100 μM histamine (*Hist.*). *C*, HeLa cells transfected with cytAEQ and 2B-GFP or mt-GFP (*control*) were incubated in Ca^{2+}-free medium (plus 100 μM EGTA) and challenged with histamine, followed by the addition of Ca^{2+}-containing medium. Representative traces in $[Ca^{2+}]_{mt}$ (*A*) and $[Ca^{2+}]_{cyt}$ (*B*) in 2B-expressing cells (*gray line*) and control cells (*black line*) are shown on the *left*. On the *right* is shown the average ± S.D. of six independent experiments. *, $p < 0.005$.

i.e. the higher the initial $[Ca^{2+}]_{cyt}$, the lower the amount of Ca^{2+} that can be released from the stores (Fig. 1, *C* and *D*). Fig. 1*D* also demonstrates that the filling state of the thapsigargin-sensitive stores of 2B-GFP-expressing cells was always lower than that of control cells, even when the initial $[Ca^{2+}]_{cyt}$ was similar. Taken together, these results show that the 2B-induced reduction in the $[Ca^{2+}]$ of the stores precedes the increased influx of extracellular Ca^{2+}, providing evidence that the stores are the primary target of 2B.

Reduced ER and Golgi Luminal Ca^{2+} Concentrations in 2B-expressing Cells—To investigate the effect of 2B on ER and Golgi calcium levels directly and independently, we used chimeras of aequorin, a Ca^{2+}-sensitive photoprotein. To this end, HeLa cells were cotransfected with erAEQ or GoAEQ and 2B-GFP or mt-GFP (which was further used as negative control throughout this study), and the $[Ca^{2+}]_{ER}$ and $[Ca^{2+}]_{Golgi}$ were compared. To efficiently reconstitute the aequorin chimeras and reliably measure $[Ca^{2+}]_{ER}$ and $[Ca^{2+}]_{Golgi}$, the luminal $[Ca^{2+}]$ of these organelles must first be reduced. This was obtained by incubation of the cells in KRB supplemented with coelenterazine (*i.e.* the prosthetic group of aequorin) and ionomycin, a Ca^{2+} ionophore, in the absence of extracellular Ca^{2+}. Aequorin luminescence signals were collected using a luminometer and calibrated into $[Ca^{2+}]$ values. Under these conditions, the $[Ca^{2+}]$ was <10 μM in both organelles. Upon switching the perfusion medium to KRB buffer supplemented with 1 mM Ca^{2+}, $[Ca^{2+}]_{ER}$ and $[Ca^{2+}]_{Golgi}$ gradually increased, reaching plateau levels in control cells of ~365 μM in the ER and ~345 μM in the Golgi (Fig. 2). In 2B-GFP-expressing cells, lower steady state levels (~30–40% reduction) were observed in both compartments (~255 and ~215 μM in the ER and Golgi, respectively). The addition of histamine to the cells resulted in a rapid decrease in $[Ca^{2+}]$ in both organelles, confirming that the sensitivity to agonists of the two Ca^{2+} stores was retained, although a smaller amount of Ca^{2+} could be released in 2B-expressing cells. Taken together, these data indicate that 2B is responsible for a reduction of the luminal $[Ca^{2+}]$ in both ER and Golgi.

Mitochondrial and Cytosolic Ca^{2+} Handling in 2B-expressing Cells—Mitochondria play an important role in intracellular Ca^{2+} homeostasis. The mitochondria are localized in close proximity of inositol 1,4,5-trisphosphate (IP3)-gated channels and are capable of taking up the Ca^{2+} that is released by IP3-generating agonists, thereby buffering the $[Ca^{2+}]_{cyt}$ (35). We hypothesized that the 2B-induced reduction in the steady state $[Ca^{2+}]_{ER}$ and $[Ca^{2+}]_{Golgi}$ levels and the ensuing reduction of IP3-induced Ca^{2+} release should decrease the uptake of Ca^{2+} by the mitochondria. To test this hypothesis, HeLa cells were transfected with mtAEQ and either 2B-GFP or mt-GFP and then challenged with histamine (in the presence of extracellular Ca^{2+}). Fig. 3*A* shows that the peak mitochondrial response is markedly reduced (almost ~35%) in 2B-GFP-expressing cells compared with the control cells. Similar results were obtained when cells were challenged with ATP, an agonist that drives production of IP3 through its action on a Gq-coupled P2Y receptor, or when CHO cells were used as model system (data not shown). Taken together, these data indicate that the 2B-induced reduction of $[Ca^{2+}]$ in the stores leads to a reduction in the stimulus-induced mitochondrial Ca^{2+} uptake.

The 2B-induced reduction in the steady state $[Ca^{2+}]_{ER}$ and

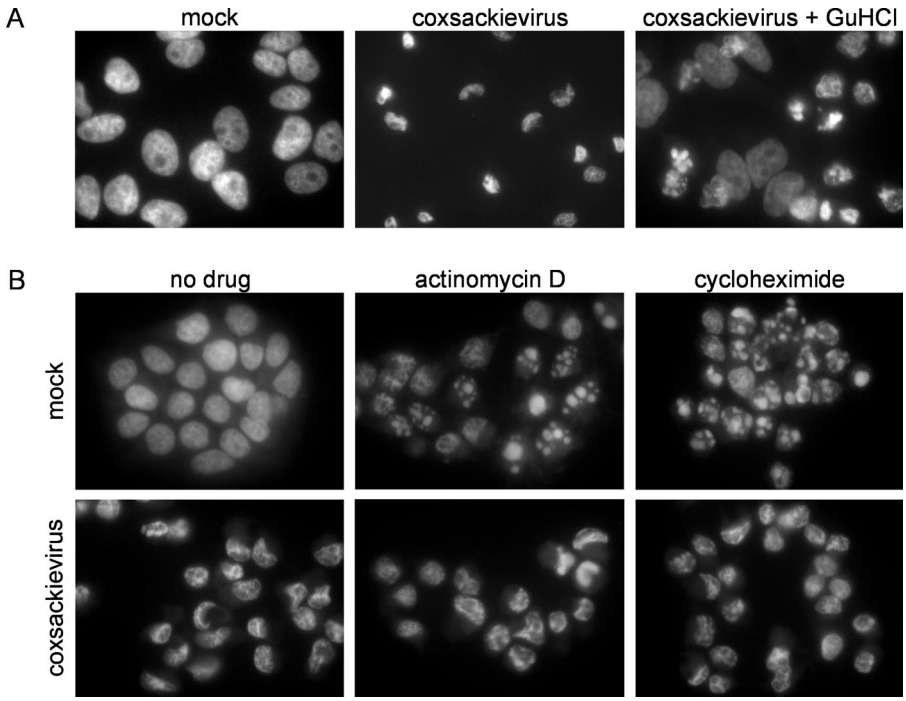

FIG. 4. **Coxsackieviruses confer an antiapoptotic state to infected cells.** *A*, coxsackievirus-induced cell death upon permissive and nonpermissive infection. HeLa cells were either mock-infected (*left*) or infected with coxsackievirus at an multiplicity of infection of 50 in the absence (*middle*) or presence (*right*) of 2 mM GuHCl and then incubated at 37 °C. At 14 h postinfection, cells were fixed, and the nuclei were stained with DAPI. The addition of 2 mM GuHCl to noninfected cells had no toxic effect on the cells (data not shown). *B*, coxsackievirus infection protects against actinomycin D and cycloheximide-induced apoptosis. HeLa cells were mock-infected (*upper row*) or infected with coxsackievirus (*bottom row*), grown at 37 °C, and, after 4 h, either mock-treated (*left*) or treated with actinomycin D (0.5 μg/ml; *middle*) or cycloheximide (100 μg/ml; *right*) for 4 h. At the end of the experiment, cells were fixed, and the nuclei were stained with DAPI. One representative experiment of three independent experiments is shown.

$[Ca^{2+}]_{Golgi}$ levels should also be reflected in a decrease in the rise of the $[Ca^{2+}]_{cyt}$ upon stimulation with IP3-generating agonists. To investigate this supposition, HeLa cells were cotransfected with cytAEQ and 2B-GFP or mt-GFP and then challenged with histamine (in the presence of extracellular Ca^{2+}). Surprisingly, we found no difference in the amplitude of $[Ca^{2+}]_{cyt}$ between 2B-GFP-expressing cells and control cells (Fig. 3*B*). On the contrary, upon releasing Ca^{2+} from the stores by a passive process (*i.e.* ionomycin treatment in Ca^{2+}-free conditions), a significant reduction in 2B-GFP-expressing cells was observed (data not shown). A likely explanation for the results shown in Fig. 3*B* is that a reduced amount of Ca^{2+} is released by histamine in 2B-GFP-expressing cells but that this effect is masked by an increased influx of Ca^{2+} from the extracellular medium due to an additional effect of 2B. To find support for this hypothesis, we evaluated the relative efficiency of the two pathways in HeLa and CHO cells for Ca^{2+} increase in the cytosol; *i.e.* the Ca^{2+} released from stores and Ca^{2+} influx from the extracellular medium. In these experiments, the cells were first challenged with histamine in HeLa (or ATP in CHO) in Ca^{2+}-free medium; under those conditions the increase of the $[Ca^{2+}]_{cyt}$ will be due only to the release of Ca^{2+} from the stores. The following re-addition of Ca^{2+} to the extracellular medium causes a second $[Ca^{2+}]_{cyt}$ rise due to the influx through the plasma membrane channels. Fig. 3*C* demonstrates that an increased influx of Ca^{2+} in 2B-expressing cells indeed equilibrates the reduced amount of Ca^{2+} that is released from the stores in these cells as compared with control cells.

Coxsackievirus Infection Protects against Cycloheximide and Actinomycin D-induced Apoptosis—Poliovirus infection of HeLa cells under permissive conditions results in CPE, whereas infection under nonpermissive conditions (*e.g.* in the presence of GuHCl, an inhibitor of viral replication) results in apoptotic cell death (4). Moreover, productive poliovirus infection has been shown to confer an antiapoptotic state to HeLa cells that protects them against apoptosis induced by actinomycin D and cycloheximide (at concentrations of 0.5 μg/ml and 100 μg/ml, respectively) (4). We tested whether these features are conserved in coxsackievirus. HeLa cells were infected with coxsackievirus in the absence or presence of GuHCl, and the type of cell death that was induced was assayed by examining the nuclear morphology. Fig. 4*A* shows that the productive coxsackievirus infection of HeLa cells (*i.e.* in the absence of GuHCl) resulted in the canonical CPE (crescent-shaped nuclei with condensed chromatin), whereas under nonpermissive conditions (*i.e.* in the presence of absence of GuHCl) a typical nuclear apoptotic response, *i.e.* condensation of chromatin and fragmentation into apoptotic bodies, was observed in a large portion of the cells, similarly as described for poliovirus (4). To test whether coxsackievirus also initiates an antiapoptotic program, mock-infected and coxsackievirus-infected cells were challenged with actinomycin D and cycloheximide in the concentrations described above. Fig. 4*B* shows that treatment of mock-infected cells with these drugs resulted in a typical nuclear apoptotic response. Upon the addition of these drugs to coxsackievirus-infected cells, however, no signs of apoptosis were observed, but signs typical of CPE were manifested instead. Together, these findings suggest that the antiapoptotic function is conserved in coxsackievirus.

To further demonstrate the existence of a viral antiapoptotic function, we monitored the ability of coxsackievirus to suppress caspase activation. To this end, HeLa cells that were either mock-infected or coxsackievirus-infected were treated with actinomycin D. Caspase activation was monitored both by incubating HeLa cell lysates with a caspase-3 fluorescent substrate and by analyzing internucleosomal DNA degradation ("laddering"). Fig. 5 shows that both caspase activation and DNA laddering are strongly reduced in coxsackievirus-infected cells.

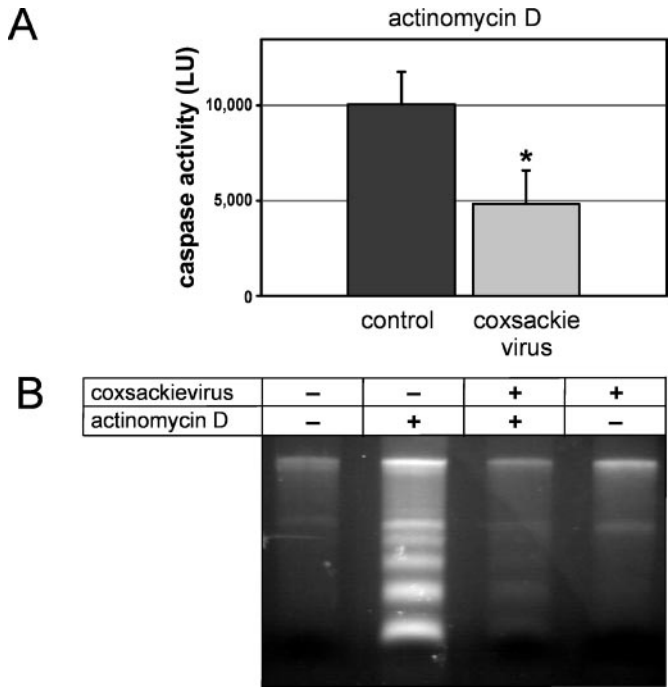

FIG. 5. **Suppression of caspase-3 activation in coxsackievirus-infected cells.** HeLa cells were mock-infected or infected with coxsackievirus at an multiplicity of infection of 50. After 1 h, cells were treated with actinomycin D (0.5 μg/ml) for 4 h and then subjected to analysis of caspase-3 activity (*A*) or DNA laddering (*B*). In *panel A*, the average ± S.D. of three independent measurements is shown (values are corrected for the background caspase-3 activity observed in control cells). *, $p < 0.05$. One representative experiment of three independent experiments is shown. *LU*, light units.

These findings provide further evidence for the existence of an antiapoptotic function in coxsackievirus.

Expression of 2B Protects against Cycloheximide and Actinomycin D-induced Apoptosis—Next, the possible role of the coxsackievirus 2B-induced alterations in Ca^{2+} homeostasis in the suppression of apoptosis was investigated. For this investigation the following protocol was used. Cells were transfected with 2B-GFP, and the number of fluorescent cells was counted at the microscope before and after a challenge with an apoptotic drug. The rationale, as reported previously for other proteins such as Bcl-2 (36) and VDAC (37), is that if the transfected protein increases the sensitivity to apoptotic agents, the number of fluorescent cells will be lower after the apoptotic challenge (because more transfected cells die), whereas the opposite will happen if the protein has antiapoptotic activity.

To investigate whether 2B is involved in conferring an antiapoptotic state to infected cells, 2B-GFP-expressing cells and mt-GFP-expressing cells were challenged with actinomycin D and cycloheximide at 36 h posttransfection. The results obtained with actinomycin D are shown in Fig. 6*A*. When mt-GFP was transfected, ~40–45% of the cells showed GFP fluorescence. 16 h after the addition of actinomycin D, the number of viable cells was drastically reduced, but the fraction of fluorescent cells remained the same. Conversely, when 2B-GFP was transfected, the same fraction of fluorescent cells was identified before actinomycin D treatment, but it markedly increased 16 h after the addition of the apoptotic agent (~70%). These data indicate that the 2B-induced alterations in Ca^{2+} homeostasis confer protection against actinomycin D-induced apoptotic cell death ($p < 0.005$). Enhanced survival was also observed upon treatment with cycloheximide ($p < 0.01$) (Fig. 6*B*).

To test whether the expression of 2B also protects against other apoptotic stimuli, we tested the possible suppressive effect against apoptosis induced by 10 μM ceramide, a lipid signaling mediator that releases Ca^{2+} from intracellular stores and induces apoptosis via a Bcl-2 sensitive pathway (38), and by 20 μM etoposide, a drug that causes DNA damage by inhibiting topoisomerase II, leading to apoptosis through p53 via a Bcl-2-sensitive, Bax-dependent pathway. Again, the number of fluorescent cells before and after a treatment with the apoptotic drugs was determined. No change in the percentage of living fluorescent cells was observed in HeLa cells transfected with mt-GFP. Cells expressing 2B-GFP were efficiently protected against apoptosis induced by ceramide ($p < 0.005$) (Fig. 6*C*) but not by etoposide (Fig. 6*D*). The failure of 2B to suppress etoposide-induced apoptosis was not due to a lower apoptotic efficacy of this drug (etoposide induced apoptosis in ~60% of the cells, similar to what was observed for actinomycin D and cycloheximide; data not shown). Taken together, these data indicate that 2B protects against some, but not all, Bcl-2-sensitive apoptotic pathways.

To demonstrate that the cytoprotective effect of 2B is indeed due to a reduced activation of caspases, cells expressing either 2B-GFP or mt-GFP were treated either with actinomycin D, cycloheximide, or etoposide and then stained with an antibody that specifically recognizes the active form of caspase-3 but not its inactive zymogen (Fig. 7). In control cells, the vast majority of cells showed extensive caspase-3 activation upon the addition of each of these apoptotic drugs (similarly as in nontransfected cells; data not shown). In 2B-expressing cells, however, caspase-3 activation induced by actinomycin D and cycloheximide, but not by etoposide, was potently suppressed. These findings are in agreement with the results described in Fig. 6 and provide evidence that the enhanced survival observed in 2B-expressing cells is due to the suppression of caspase-3 activation.

Effects on Intracellular Ca^{2+} Homeostasis and Apoptosis of 2B Mutants—Our data strongly suggest that the 2B protein lends protection against apoptosis through its ability to manipulate intracellular Ca^{2+} homeostasis. However, it cannot be excluded that the effects of 2B on Ca^{2+} homeostasis and its anti-apoptotic ability represent two distinct, unrelated functions. To investigate whether the antiapoptotic activity of 2B is functionally related to its ability to manipulate intracellular Ca^{2+} fluxes, we characterized two 2B-GFP mutants with mutations in the hydrophobic regions that are implicated in pore formation (17). In the first mutant, the amphipathic character of the α-helix formed by the first hydrophobic region (aa 37–54) is disturbed by the substitution of lysine residues 41, 44, and 48 with hydrophobic leucine residues (mutation K41L/K44L/K48L) (25). In the second mutant, the hydrophobic nature of the second hydrophobic region (aa 63–80) is disturbed by substitution of two hydrophobic residues (isoleucine 64 and valine 66) by polar serine residues (mutation I64S/V66S) (20).

HeLa cells were cotransfected with erAEQ and the indicated 2B-GFP mutants or mt-GFP, and the $[Ca^{2+}]_{ER}$ was compared. Fig. 8*A* shows that both mutants 2B-K41L/K44L/K48L and 2B-I64S/V66S failed to reduce the luminal $[Ca^{2+}]$ in the ER. Consistent with this, measurement of the $[Ca^{2+}]_{mt}$ upon challenge with histamine in cells transfected with mtAEQ showed that the peak mitochondrial Ca^{2+} response in cells expressing the mutants was similar to that in control cells (Fig. 8*B*). These data provide evidence that both mutants are defective in manipulating intracellular Ca^{2+} fluxes. To investigate the antiapoptotic activity of these mutants, HeLa cells expressing the 2B-GFP mutants were challenged with either actinomycin D or cycloheximide, and caspase-3 activation was analyzed as described above. Fig. 9 shows that the mutants 2B-K41L/K44L/K48L and 2B-I64S/V66S were unable to suppress either acti-

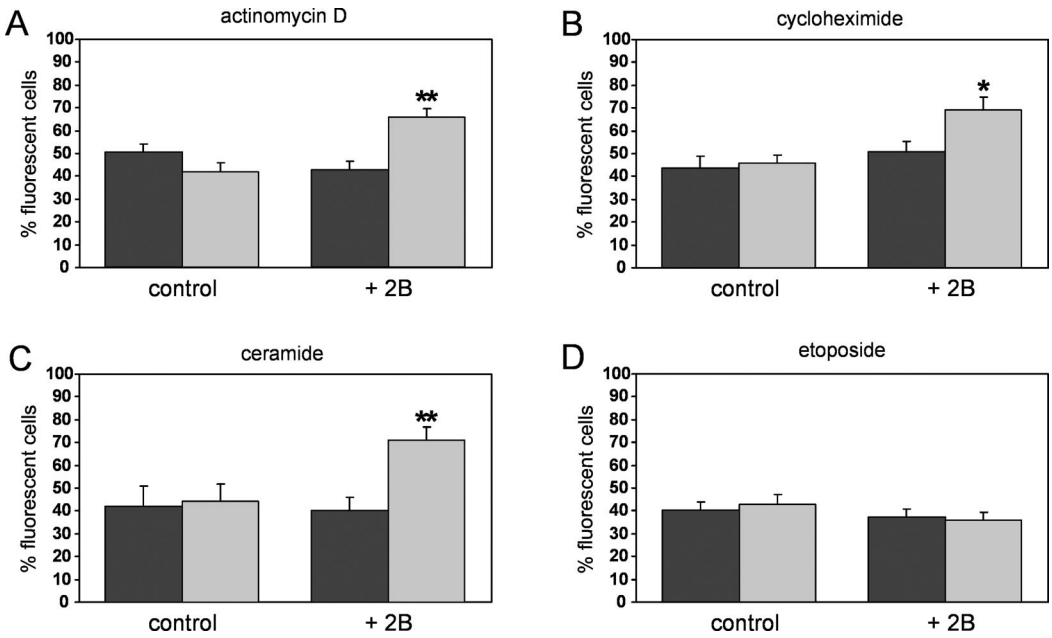

FIG. 6. **Protein 2B protects against apoptotic cell death induced by actinomycin D, cycloheximide, and ceramide, but not etoposide.** HeLa cells were transfected with 2B-GFP or mt-GFP (control). At 36 h posttransfection, cells were either mock-treated (*dark gray*) or treated (*light gray*) with actinomycin D (0.5 μg/ml) (*A*), cycloheximide (100 μg/ml) (*B*), ceramide (10 μM) (*C*), or etoposide (20 μM) (*D*) for 16 h. The percentage of fluorescent cells before and after the challenge with the apoptotic drugs was determined *de visu* by counting at the microscope. The average ± S.D. of four independent experiments is shown. *, $p < 0.01$; **, $p < 0.005$.

nomycin D-induced or cycloheximide-induced caspase-3 activation. Consistent with this, both mutants also failed to increase cell survival after treatment with these apoptotic drugs (data not shown). Together, these findings demonstrate that the antiapoptotic activity of 2B is functionally linked to its ability to manipulate intracellular Ca^{2+} homeostasis.

DISCUSSION

Viruses induce a number of alterations in the metabolism and structure of their host cell to ensure efficient reproduction. Some of these alterations can be sensed by the host cell and turn on a defensive apoptotic reaction that is aimed at curtailing virus replication. Many viruses have developed countermeasures to prevent premature abortion of the viral life cycle. Enteroviruses are small cytolytic RNA viruses that cause a necrosis-like type of cell death, called CPE, which is the ultimate result of a complex interplay between apoptosis-inducing and apoptosis-suppressing functions encoded by the enterovirus genome (4). In this report, we provide evidence that the enterovirus 2B protein plays a major role in suppressing apoptotic host cell responses by manipulating intracellular Ca^{2+} homeostasis.

Using both chemical and genetically encoded Ca^{2+} indicators, we demonstrated that the expression of 2B results in the following effects: (i) a reduction in the luminal $[Ca^{2+}]$ in both ER and Golgi; (ii) a decrease in the amount of Ca^{2+} that can be released from these organelles using either thapsigargin or physiological, IP3-generating stimuli like histamine and ATP; (iii) a reduction in the stimulus-induced amount of Ca^{2+} that is taken up by mitochondria; and (iv) an increase in the influx of extracellular Ca^{2+}, leading to a rise in $[Ca^{2+}]_{cyt}$. The reduction in the Ca^{2+}-filling state of the stores preceded the increase in the influx of extracellular Ca^{2+}, indicating that the stores are the primary target of 2B. Similar results were obtained in HeLa cells and CHO cells, indicating that it is unlikely that the effects of 2B are cell type-specific. These data are consistent with the idea that 2B decreases $[Ca^{2+}]_{ER}$ and $[Ca^{2+}]_{Golgi}$ by increasing the passive leakage of Ca^{2+} ions from these stores, most likely through the formation of membrane-integral pores, and thereby accounts for a reduction in the amount of releasable Ca^{2+} and the down-regulation of Ca^{2+} fluxes between stores and the mitochondria. The increased influx of Ca^{2+} is most likely due to the increased plasma membrane permeability that is observed in 2B-expressing cells, which allows the passage of ions and normally nonpermeant low molecular weight compounds (11, 39, 40).

The 2B-induced perturbation of intracellular Ca^{2+} distribution and signaling was identified as an important component of the enteroviral strategy to suppress infection-limiting apoptotic host cell responses. These apoptotic responses are most likely triggered by the action of the viral proteinases $3C^{pro}$ and $2A^{pro}$, which inhibit cellular transcription and cap-dependent translation, respectively (8, 9). Enteroviruses interrupt this apoptotic program by encoding functions that implement an antiapoptotic program (4). The antiapoptotic state that is conferred to infected cells can even suppress nonviral apoptotic stimuli such as cycloheximide and actinomycin D (whose effects resemble those of $3C^{pro}$ and $2A^{pro}$, respectively). In our studies of the physiological relevance of the 2B-induced alterations in intracellular Ca^{2+} homeostasis, we observed a role for 2B in suppressing apoptosis. The expression of 2B suppressed caspase-3 activation and apoptotic cell death induced by actinomycin D and cycloheximide. Mutants of 2B that were defective in manipulating intracellular Ca^{2+} fluxes failed to protect against apoptosis. Together, these findings strongly suggest that 2B, by modulating intracellular Ca^{2+} homeostasis, plays a major role in conferring the antiapoptotic state to infected cells and, thereby, in extending the life span of the host cell.

The enterovirus 2B protein represents one of the first antiapoptotic proteins of small genome RNA viruses. Most of our knowledge about viral apoptosis-suppressing functions comes from the group of large genome DNA viruses (herpesviruses, adenoviruses, and poxviruses), which often encode multiple antiapoptotic proteins, including Bcl-2 homologs, caspase suppressors, and cell cycle and transcription mediators (1, 2). Relatively little is known about apoptosis-suppressing functions in small genome RNA viruses that exhibit a relatively fast

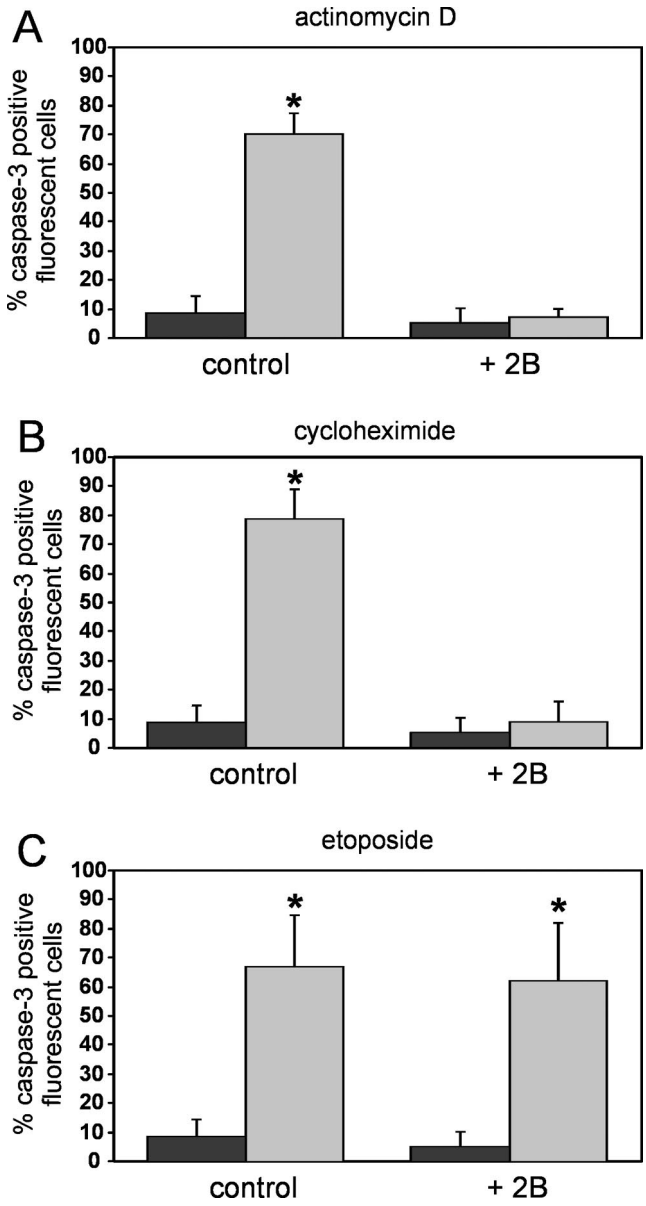

FIG. 7. **Protein 2B suppresses caspase-3 activation induced by actinomycin D and cycloheximide.** HeLa cells were transfected with 2B-GFP or mt-GFP (control). At 36 h posttransfection, cells were either mock-treated (*dark gray*) or treated (*light gray*) with actinomycin D (0.5 μg/ml) (*A*), cycloheximide (100 μg/ml) (*B*), ceramide (10 μM) (*C*), or etoposide (20 μM) (*D*) for 4 h. Cells were fixed and stained with an anti-active caspase-3 antibody. The percentage of caspase-3-positive GFP-expressing cells was determined *de visu* by counting at the microscope. The average ± S.D. of three independent experiments is shown. *, $p < 0.005$.

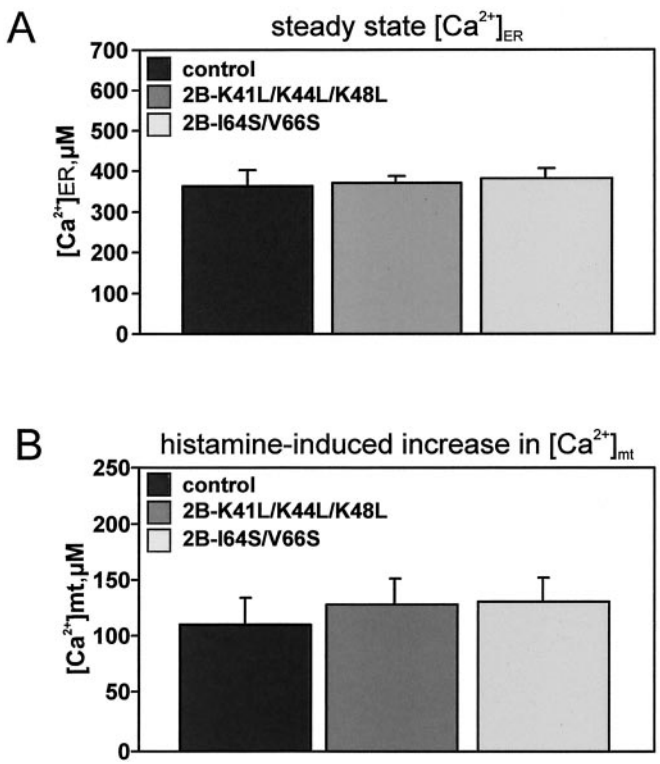

FIG. 8. **Mutants 2B-K41L/K44L/K48L and 2B-I64S/V66S do not alter intracellular Ca^{2+} homeostasis.** Measurement of the steady-state $[Ca^{2+}]_{ER}$ (*A*) and the histamine-induced increase in $[Ca^{2+}]_{mt}$ (*B*) were performed as described in the legends of Figs. 2 and 3, respectively.

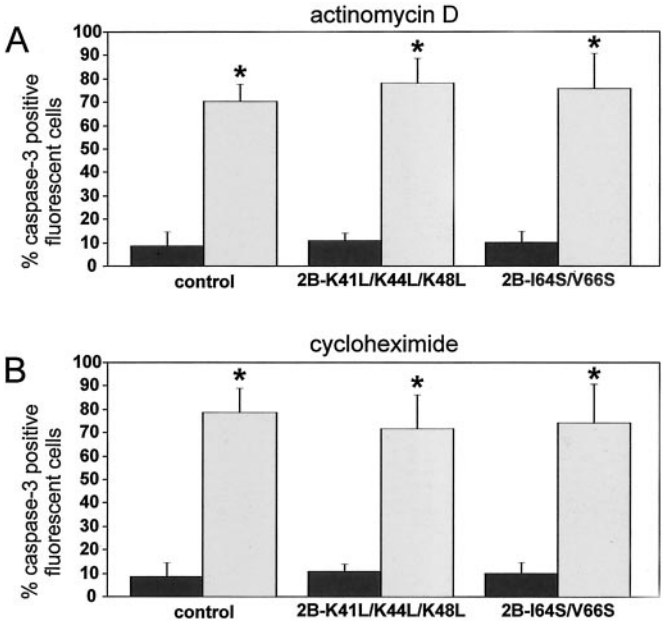

FIG. 9. **Mutants 2B-K41L/K44L/K48L and 2B-I64S/V66S fail to suppress actinomycin D-induced and cycloheximide-induced apoptosis.** Analysis of the caspase-3 activation induced by actinomycin D (*A*) or cycloheximide (*B*) was performed as described in the legend of Fig. 7.

replication cycle and have little, if any, genetic capacity to develop individual antiapoptotic functions. It has been suggested that the antiapoptotic activities of RNA viruses may be byproducts of the cellular alterations that are induced by the viral replication proteins to efficiently replicate their RNA genome. Obviously, the ability of 2B to suppress apoptotic host cell responses is not its sole or primary function. Mutations in the hydrophobic domains of 2B, which most likely interfere with pore formation (as shown in this study for the mutants 2B-K41L/K44L/K48L and 2B-I64S/V66S), cause primary defects in viral RNA replication (20, 21). The exact function of 2B is as yet unknown. The ability of 2B to form pore-like structures in secretory pathway membranes may be required for the ability of the 2BC precursor to cause the accumulation of secretory pathway-derived membrane vesicles at which viral RNA replication takes place (3, 41). Thus, the ability of 2B to reduce the Ca^{2+} filling state of the stores most likely serves two different functions, namely formation of the viral replication complex and suppression of apoptotic host cell responses.

How can the 2B-induced alterations in intracellular Ca^{2+}

signaling lend protection against certain apoptotic stimuli? The finding that 2B failed to suppress etoposide-induced apoptosis indicates that the alterations in Ca^{2+} homeostasis suppress a specific apoptotic pathway rather than confer a general blockage of apoptosis. Recent studies on the Bcl-2 oncogene have provided evidence for the coexistence of spatially different apoptotic pathways in the same cell, one ER-dependent and one mitochondrion-dependent, which eventually converge at the mitochondria (42, 43). Bcl-2 is localized at the outer mitochondrial membrane, the nuclear envelope, and the ER membrane. Most of the results published so far have emphasized the importance of Bcl-2 at the mitochondria, where it antagonizes the ability of pro-apoptotic Bcl-2 family members to induce cytochrome C release (44). The function of Bcl-2 at the ER membrane is less clear. An ER-restricted Bcl-2 mutant suppressed apoptosis induced by various stimuli (including ceramide) but failed to protect against etoposide, a drug that acts directly at the mitochondria by causing membrane translocation of Bax (42, 43). The antiapoptotic activity of ER-restricted Bcl-2 argues for the existence of a signaling mechanism between the ER and the mitochondria. Growing evidence indicates that alterations in Ca^{2+} fluxes between these organelles have a modulatory effect on apoptosis (13). Key events occurring in the mitochondrial matrix such as ATP production, an important source of reactive oxygen species production, and possibly also the opening of the permeability transition pore leading to swelling of the outer mitochondrial membrane and the release of proapoptotic proteins like cytochrome C, are sensitive to increases in $[Ca^{2+}]_{mt}$ (13, 45). Accordingly, down-regulation of Ca^{2+} fluxes between the ER and the mitochondria can protect the mitochondria from cytotoxic rises in $[Ca^{2+}]_{mt}$. Increasing evidence indicates that Bcl-2 exerts some of its antiapoptotic effects from the ER by reducing $[Ca^{2+}]_{ER}$ and down-regulating Ca^{2+} fluxes between the ER and mitochondria (36, 46, 47), possibly through the ability of Bcl-2 to form ion channels in the ER membrane (48). Moreover, conditions that lowered $[Ca^{2+}]_{ER}$ protected HeLa cells from ceramide-induced apoptosis, whereas conditions that increased $[Ca^{2+}]_{ER}$ had the opposite effect (38). The findings that 2B down-regulated Ca^{2+} fluxes between the stores and the mitochondria and suppressed apoptosis induced by ceramide, but not etoposide, strongly suggest that 2B specifically targets a Ca^{2+}-sensitive, ER-dependent apoptotic pathway.

Is the ability of 2B to decrease Ca^{2+} signaling between the ER and mitochondria sufficient for conferring an antiapoptotic state to enterovirus-infected cells? In both poliovirus-infected cells (4, 6) and coxsackievirus-infected cells (this study), the antiapoptotic function is expressed early in the infection (*i.e.* at ~2 h postinfection). Previously, we demonstrated that coxsackievirus infection results in a ~50% reduction of the Ca^{2+} content of the thapsigargin-sensitive stores within the first 2 h of infection (15). Thus, the virus-induced alterations in intracellular Ca^{2+} signaling coincide with the implementation of the anti-apoptotic state, lending support to the idea that these events are causally linked. It cannot be excluded that the rise in $[Ca^{2+}]_{cyt}$ also contributes somehow to the suppression of apoptosis in infected cells. A rise in $[Ca^{2+}]_{cyt}$ may lead to the activation of calpains, Ca^{2+}-sensitive proteases that can exert antiapoptotic effects by cleaving caspases, including key caspases 8 and 9 (49, 50). Interestingly, aberrant processing of caspase-9 (albeit at a low level) was observed in HeLa cells upon productive poliovirus infection but not upon abortive infection (51). However, aberrant processing of caspase-9 was not reported upon productive coxsackievirus infection (52). Our observation that the 2B-induced alterations in Ca^{2+} homeostasis failed to protect against etoposide-induced caspase-9-dependent apoptosis suggests that it is unlikely that aberrant processing of caspase-9 can completely account for the anti-apoptotic activity of 2B. Moreover, significant rises in $[Ca^{2+}]_{cyt}$ of coxsackievirus-infected cells take place only after 5 h. Therefore, we propose that the 2B-induced reduction of the Ca^{2+} content of the ER and Golgi and the resulting down-regulation of Ca^{2+} fluxes between these stores and the mitochondria is the major component of the viral antiapoptotic program. It should be kept in mind, however, that signs of apoptosis (cytochrome C release and caspase activation) become apparent in enterovirus-infected cells (7, 51, 52) later in the infection, and it has been suggested that this may contribute to the killing of the host cell and the release of virus progeny (52). Thus, the antiapoptotic activity of the 2B protein most likely serves to delay apoptotic responses, thereby providing the virus the time required for genome replication, rather than to completely prevent all signs of apoptosis.

Further research is required to define the antiapoptotic mechanism of 2B and the role of Ca^{2+} therein. A better understanding of the molecular mechanism used by enteroviruses to manipulate cell death may lead to a better insight into the pathogenesis of viral disease and may contribute to our understanding of the critical role of Ca^{2+} signaling in the modulation of apoptosis.

Acknowledgment—We thank Jeroen van Kilsdonk for technical assistance with the Fura-2 experiments.

REFERENCES

1. O'Brien, V. (1998) *J. Gen. Virol.* **79,** 1833–1845
2. Hay, S., and Kannourakis, G. (2002) *J. Gen. Virol.* **83,** 1547–1564
3. Bienz, K., Egger, D., and Pfister, T. (1994) *Arch. Virol. Suppl.* **9,** 147–157
4. Tolskaya, E. A., Romanova, L. I., Kolesnikova, M. S., Ivannikova, T. A., Smirnova, E. A., Raikhlin, N. T., and Agol, V. I. (1995) *J. Virol.* **69,** 1181–1189
5. Agol, V. I., Belov, G. A., Bienz, K., Egger, D., Kolesnikova, M. S., Raikhlin, N. T., Romanova, L. I., Smirnova, E. A., and Tolskaya, E. A. (1998) *Virology* **252,** 343–353
6. Agol, V. I., Belov, G. A., Bienz, K., Egger, D., Kolesnikova, M. S., Romanova, L. I., Sladkova, L. V., and Tolskaya, E. A. (2000) *J. Virol.* **74,** 5534–5541
7. McCarthy, C. M., Granville, D. J., Watson, K. A., Anderson, D. R., Wilson, J. E., Yang, D., Hunt, D. W. C., and McManus, B. M. (1998) *J. Virol.* **72,** 7669–7675
8. Barco, A., Feduchi, E., and Carrasco, L. (2000) *Virology* **266,** 352–360
9. Goldstaub, D., Gradi, A., Bercovitch, Z., Grosmann, Z., Nophar, Y., Luria, S., Sonenberg, N., and Kahana, C. (2000) *Mol. Cell. Biol.* **20,** 1271–1277
10. Neznanov, N., Kondratova, A., Chumakov, K., Angres, B., Zhumabayeva, B., Agol, V. I., and Gudkov, A. V. (2001) *J. Virol.* **75,** 10409–10420
11. Doedens, J. R., and Kirkegaard, K. (1995) *EMBO J.* **14,** 894–907
12. Berridge, M. J., Lipp, P., and Bootman, M. D. (2000) *Nat. Rev. Mol. Cell. Biol.* **1,** 11–21
13. Orrenius, S., Zhivotovsky, B., and Nicotera, P. (2003) *Nat. Rev. Mol. Cell Biol.* **4,** 552–565
14. Irurzun, A., Arroyo, J., Alvarez, A., and Carrasco, L. (1995) *J. Virol.* **69,** 5142–5146
15. van Kuppeveld, F. J. M., Hoenderop, J. G. J., Smeets, R. L. L. M., Willems, P. H. G. M., Dijkman, H. B. P. M., Galama, J. M. D., and Melchers, W. J. G. (1997) *EMBO J.* **16,** 3519–3532
16. Aldabe, R., Irurzun, A., and Carrasco, L. (1997) *J. Virol.* **71,** 6214–6217
17. de Jong, A. S., Wessels, E., Dijkman, H. B. P. M., Galama, J. M. D., Melchers, W. J. G., Willems, P. H. G. M., and van Kuppeveld, F. J. M. (2003) *J. Biol. Chem.* **278,** 1012–1021
18. Schlegel, A., Giddings, T. H., Jr., Ladinsky, M. L., and Kirkegaard, K. (1996) *J. Virol.* **70,** 6576–6588
19. Rust, R. C., Landmann, L., Gosert, R., Tang, B. L., Hong, W., Hauri, H. P., Egger, D., and Bienz, K. (2001) *J. Virol.* **75,** 9808–9818
20. van Kuppeveld, F. J. M., Galama, J. M. D., Zoll, J., and Melchers, W. J. G. (1995) *J. Virol.* **69,** 7782–7790
21. van Kuppeveld, F. J. M., Galama, J. M. D., Zoll, J., van den Hurk, P. J. J. C., and Melchers, W. J. G. (1996) *J. Virol.* **70,** 3876–3886
22. Segrest, J. P., de Loof, H., Dohlman, J, G., Brouillette, C. G., and Anantharamaiah, G. M. (1990) *Proteins* **8,** 103–117
23. Shai, Y. (1999) *Biochim. Biophys. Acta* **1462,** 55–70
24. Cuconati, A., Xiang, W., Lasher, F., Pfister, T., and Wimmer, E. (1998) *J. Virol.* **72,** 1297–1307
25. de Jong, A. S., Schrama, I. W. J., Willems, P. H. G. M., Galama, J. M. D., Melchers, W. J. G., and van Kuppeveld, F. J. M. (2002) *J. Gen. Virol.* **83,** 783–793
26. Agirre, A., Barco, A., Carrasco, L., and Nieva, J. L. (2002) *J. Biol. Chem.* **277,** 40434–40441
27. van Kuppeveld, F. J. M., Melchers, W. J. G., Willems, P. H. G. M., and Gadella T. W., Jr. (2002) *J. Virol.* **76,** 9446–9456
28. Rizzuto, R., Brini, M., Pizzo, P., Murgia, M., and Pozzan, T. (1995) *Curr. Biol.*

5, 635–642
29. Rizzuto, R., Simpson, A. W. M., Brini, M., and Pozzan, T. (1992) *Nature* **358,** 325–328
30. Brini, M., Marsault, R., Bastianutto, C., Alvarez, J., Pozzan, T., and Rizzuto, R. (1995) *J. Biol. Chem.* **270,** 9896–9903
31. Montero, M., Brini, M., Marsault, R., Alvarez, J., Sitia, R., Pozzan, T., and Rizzuto, R. (1995) *EMBO J.* **14,** 5467–5475
32. Pinton, P., Pozzan, T., and Rizzuto, R. (1998) *EMBO J.* **17,** 5298–5308
33. Barrero, M. J., Montero, M., and Alvarez, J. (1997) *J. Biol. Chem.* **272,** 27694–27699
34. Bolsover, S., Ibrahim, O., O'Luanaigh, N., Williams, H., and Cockcroft, S. (2001) *Biochem. J.* **356,** 345–352
35. Rizzuto, R., Pinton, P, Carrington, W., Fay, F. S., Fogarty, K. E., Lifshitz, L. M., Tuft, R. A., and Pozzan, T. (1998) *Science* **280,** 1763–1766
36. Pinton, P., Ferrari, D., Magalhaes, E., Schulze-Osthoff, K., di Virgilio, F., Pozzan, T., and Rizzuto, R. (2000) *J. Cell Biol.* **148,** 857–862
37. Rapizzi, E, Pinton, P., Szabadkai, G., Wieckowski, M. R., Vandecasteele, G., Baird, G., Tuft, R. A., Fogarty, K. E., and Rizzuto, R. (2002) *J. Cell Biol.* **159,** 613–624
38. Pinton, P., Ferrari, D., Rapizzi, E., di Virgilio, F., Pozzan, T., and Rizzuto, R. (2001) *EMBO J.* **20,** 2690–2701
39. Aldabe, R., Barco, A., and Carrasco, L. (1996) *J. Biol. Chem.* **271,** 23134–23137
40. van Kuppeveld, F. J. M., Melchers, W. J. G., Kirkegaard, K., and Doedens, J. R. (1997) *Virology* **227,** 111–118
41. Cho, M. W., Teterina, N., Egger, D., Bienz, K., and Ehrenfeld, E. (1994) *Virology* **202,** 129–145
42. Lee, S. T., Hoeflich, K. P., Wasfy, G. W., Wodgett, J. R., Leber, B, Andrews, D. W., Hedly, D. W., and Penn, L. Z. (1999) *Oncogene* **18,** 3520–3528
43. Annis, M. G., Zamzami, N., Zhu, W., Penn, L. Z., Kroemer, G., Leber, B., and Andrews, D. W. (2001) *Oncogene* **20,** 1939–1952
44. Gross, A., McDonnel, J. M., and Korsmeyer, S. (1999) *Genes Dev.* **13,** 1899–1911
45. Jouaville, L. S., Pinton, P., Bastianutto, C., Rutter, G. A., and Rizzuto, R. (1999) *Proc. Natl. Acad. Sci. U. S. A.* **96,** 13807–13812
46. Foyouzi-Youssefi, R., Arnaudeau, S., Borner, C., Kelly, W. L., Tschopp, J., Lew, D. P., Demaurex, N., and Krause, K. H. (2000) *Proc. Natl. Acad. Sci. U. S. A.* **97,** 5723–5728
47. Vanden Abeele, F., Skryma, R., Shuba, Y., Van Coppenolle, F., Slomianny, C., Roudbaraki, M., Mauroy, B., Wuytack, F., and Prevarskaya, N. (2002) *Cancer Cell* **1,** 169–179
48. Schendel, S., Xie, Z., Montal, M., Matsuyama, S., Montal, M., and Reed, J. (1997) *Proc. Natl. Acad. Sci. U. S. A.* **94,** 5113–5118
49. Chua, B. T., Guo, K., and Li, P. (2000) *J. Biol. Chem.* **275,** 5131–5135
50. Lankiewicz, S., Marc Luetjens, C., Trubc Bui, N., Krohn, A. J., Poppe, M., Cole, G. M., Saido, T. C., and Prehn, J. H. (2000) *J. Biol. Chem.* **275,** 17064–17071
51. Belov, G. A., Romanova, L. I., Tolskaya, E. A., Kolesnikova, M. S., Lazebnik, Y. A., and Agol, V. I. (2003) *J. Virol.* **77,** 45–56
52. Carthy, C. M., Yanagawa, B., Luo, H., Granville, D. J., Yang, D., Cheung, P., Esfandiarei, M., Rudin, C. M., Thompson, C. B., Hunt, D. W. C., and McManus, B. M. (2003) *Virology* **313,** 147–157